

A Flight Test to Demonstrate Flutter and Evaluate the Flutterometer

Rick Lind*

University of Florida

David F. Voracek[†] Roger Truax[‡] Tim Doyle[§] Starr Potter[¶] and Marty Brenner^{||}
NASA Dryden Flight Research Center

submitted to *The Aeronautical Journal* on May 2, 2002

*Corresponding Author, Assistant Professor, Department of Aerospace Engineering, 231 Aerospace Building, University of Florida, Gainesville FL, 32611, rick@aero.ufl.edu

[†]david.voracek@dfrc.nasa.gov

[‡]roger.truax@dfrc.nasa.gov

[§]tim.doyle@dfrc.nasa.gov

[¶]starr.potter@dfrc.nasa.gov

^{||}martin.brenner@dfrc.nasa.gov

Abstract

A project was recently completed that investigated the ability to predict the onset of flutter using tools like the flutterometer. This project used an experiment called the Aerostructures Test Wing that was flown while mounted to the Flight Test Fixture on an F-15. Several flight tests were conducted to expand the envelope and determine the aeroelastic dynamics of the experiment. The final flight ended with destruction of the experiment due to the onset of flutter. The flutterometer attempted to predict this onset by analyzing the flight data. The results indicate the flutterometer is able to generate a conservative estimate of the flight conditions associated with flutter. This paper details the flight tests of the experiment and the resulting predictions from the flutterometer.

1 Introduction

The aeroelastic phenomenon known as flutter has been around since the advent of flight¹. Indeed, the concepts associated with aeroelasticity are extensively developed and discussed in the literature^{2, 3}. Instabilities have been derived that extend well beyond the simple bending-torsion flutter into complicated mechanisms involving aeroservoelastic dynamics. Furthermore, many approaches and tools have been developed to predict the flight conditions associated with these instabilities.

The investigation of flutter through flight testing is an essential part of aircraft certification. Several methods of predicting the speeds associated with flutter have been developed and used for flight testing including extrapolating damping trends, an envelope function⁴, the Zimmerman-Weissenburger flutter margin⁵, and an identification approach⁶. Flight testing, even using these prediction methods, remains a costly and time-consuming process. The concern for flight testing is that traditional model-based and data-based approaches for predicting the onset of flutter do not provide sufficient levels of confidence and safety. Several incidents have shown that this concern is justified^{7, 8}.

A new tool has been developed to predict the onset of flutter⁹. This tool, called the flutterometer, uses a new approach called μ -method analysis to predict a robust flutter speed¹⁰. The flutterometer is significantly different from traditional prediction approaches because this tool uses both models and flight data. The resulting prediction is thus based on both theoretical dynamics of aeroelasticity and measured properties of the real aircraft.

The flutterometer needs to be extensively tested before it can be relied upon for predicting the onset of flutter during a flight test. The tool has been investigated using simulations of several systems; however, the simulated tests are always of limited value because of artificialities. The validity of the flutterometer can never be truly determined unless the simulated tests are accompanied by real tests.

Specifically, the flutterometer must be evaluated by flight testing. Some testing has been performed using wind tunnel experiments; however, those experiments could not consider issues unique to flight testing. The flutterometer must be investigated to determine the effects of issues such as modal excitation and observability, ambient noise, turbulence effects, telemetry, efficiency and computational requirements, and testing methods that are observed in actual flight environments.

NASA Dryden Flight Research Center recently completed a project that investigated the flutterometer. This project used an experiment called the Aerostructures Test Wing (ATW). The ATW was a small-scale wing structure that was flown using an F-15 and associated Flight Test Fixture.

The flight tests of the ATW were able to generate data that was used to evaluate the flutterometer. This data

included accelerometer responses to random turbulence and commanded sine sweeps. The ATW presents a particularly valuable test for the flutterometer because the exact flutter speed is known. The system actually encountered flutter during the flight test so the validity of a prediction could definitely be determined.

This paper documents the flight tests of the Aerostructures Test Wing. Various aspects of the testing are discussed. One aspect of discussion is the physical characteristics of the ATW. Another aspect of discussion is the modeling and ground testing that were performed for the ATW. Finally, the flight tests and the predictions from the flutterometer are detailed.

2 Background

2.1 Flutterometer

The flutterometer is a tool that predicts flutter margins during a flight test ⁹. This tool is inherently different from traditional approaches that attempt to predict the onset of flutter. These differences include the type of information used in the computation, the type of analysis performed by the tool, and the type of prediction that results.

Fundamentally, the flutterometer is a model-based tool. This description is intended to note that the flutter margin is computed by analyzing the stability properties of an analytical model. In this respect, the flutterometer is similar to standard computational approaches; however, the flutterometer differs with respect to how the model is formulated. The model to be analyzed actually has characteristics from both theoretical dynamics and flight data measurements. Thus, the type of information used by the flutterometer is different from other approaches.

The basis for the flutterometer is μ -method analysis ¹⁰. The μ -method analysis computes a stability measure that is robust with respect to an uncertainty description ¹¹. This uncertainty description is computed to be representative of modeling errors as noted by analyzing flight data. In this respect, the flutterometer predicts a realistic flutter speed that is more beneficial than theoretical predictions because the robust speed directly accounts for flight data. Thus, the type of analysis performed by the flutterometer is significantly different from standard aeroelastic analysis.

The flutter margin that is computed by the flutterometer is actually the robust flutter margin for the analytical model with respect to the uncertainty. This margin is mathematically valid based on the aeroelastic dynamics as indicated by the model. In this respect, the tool is analytically predictive as opposed to the *ad hoc* predictions that result from extrapolating damping trends or assumptions of general binary flutter. Thus, the type of prediction is considerably different from traditional approaches.

2.2 Flight Test Fixture for the F-15

A facility has been developed by NASA Dryden Flight Research Center that allows flight testing of various types of experiments ¹². This facility is composed of an F-15 with an associated Flight Test Fixture. In this case, the F-15 is a standard 2-seat variant of the fighter aircraft and the Flight Test Fixture is the second-generation version of a basic concept.

The Flight Test Fixture is essentially an aircraft store that is used to host experiments. This store is a thin rectangular body with an elliptical nose and blunt tail. The dimensions are 107 *in* long by 32 *in* high by 8 *in*

wide.

The main body of the Flight Test Fixture is of primary importance for flutter experiments. This body is the rectangular piece that is the largest element of the store. The main body is actually several compartmentalized sections and a set of side panels. The compartmentalized sections are used for storage of electronics such as power supplies and signal processing units. The side panels can be removed and replaced to allow external mounting of experiments.

The Flight Test Fixture mounts to the centerline pylon underneath the fuselage of the F-15 as shown in Fig. 1. The entire structure mounts behind the engine inlets in the area near the rear landing gear. This structure is similar in nature to a fuel tank that is routinely flown on the F-15 in this position; however, the Flight Test Fixture has less weight and drag and is smaller than that fuel tank. Thus, the development of the Fixture was aided by knowledge of the flight characteristics of the F-15 with a fuel tank.



Figure 1: Flight Test Fixture mounted to F-15

An airdata system is integrated into the Flight Test Fixture. This system measures angle of attack and angle of sideslip along with airspeed for the store. The angle of attack, in particular, differs between the Flight Test Fixture and the F-15 so this measurement is of concern for determining aerodynamics associated with experiments.

Extensive flight tests were performed to study the airflow around the Flight Test Fixture. Flow visualization studies have indicated that the airflow is fairly smooth around the store body for subsonic flight conditions. Shocks appear only as the F-15 approaches transonic flight and their effect seems to be concentrated towards the leading-edge portion of the structure.

Also, vibration testing was performed on this facility. Flight tests that covered a wide range of operating conditions were performed to measure accelerations. The sensors indicated noticeable responses; however, the modal frequencies of the Flight Test Fixture were above 200 Hz. Lateral motion of the structure was particularly evident but at low frequencies this motion had very low acceleration levels.

3 Experiment Issues

3.1 Objectives

A project was initially proposed in 1997 to validate the accuracy of flutter predictions. The flutterometer was of particular interest but an evaluation of traditional data-based and model-based approaches was also desired. Each of these methods had been extensively evaluated using simulated data so the next logical step was to consider flight data.

The predictions of flutter speeds were to be computed for a specially designed experiment. The main objective of this experiment was thus to provide data for analysis by the prediction approaches. Such data needed to be an extensive set of parameters that reflected the dynamical properties of the experiment.

The data used to predict flutter needed to be applicable for several types of prediction algorithms. Some algorithms use responses from random excitation whereas other algorithms use responses from a deterministic excitation. Furthermore, that deterministic excitation should include sinusoidal sweeps and dwells of different frequencies and magnitudes. An objective for the experiment could therefore be described as the generation of data in response to these particular types of excitation.

Also, the accuracy of a prediction could only be truly evaluated when the actual speed associated with flutter was known. Thus, the experiment must involve a system that incurs flutter. Data must be recorded from flight conditions ranging from stable operation to the onset of a flutter instability. The experiment did not necessarily need to actually encounter flutter; however, the testing needed to come extremely close to the instability to ensure the true flutter speed was known to a high accuracy.

Another objective of the experiment was to formulate theoretical models of the system. Computational model-based approaches were to be evaluated from several in-house and commercial software packages so a model was obviously critical. Furthermore, a model needed to be realized as a linear state-space system for use with the flutterometer.

An additional objective was associated with the basic process of flight testing. Namely, this project was to investigate the ability of engineers to monitor an experiment and safely expand the envelope near unstable flight conditions. In other words, the project should determine if the current procedures for testing provide an adequate level of safety.

3.2 Constraints

The objectives of the program could only have been satisfied by designing an experiment to undergo flight tests. Furthermore, that experiment must have been able to incur the onset of flutter. Clearly such objectives raised several concerns that translated into serious constraints and limitations for the design of the experiment.

The obvious concern for the experiment was the type of system that could be flown. The use of a real airplane to fly up to the onset of flutter was obviously too dangerous for a piloted system and too costly for an unpiloted system. Thus, the decision was made to use a scale wing to represent a realistic structure. This decision constrained the experiment to be realized as a wing with a traditional type of flutter mechanism.

The use of the F-15 with associated Flight Test Fixture presented a unique opportunity for this project. The experiment could be designed as a wing that mounted to the Flight Test Fixture. The system would be designed

such that the wing would flutter at a speed much lower than the flutter speed of the F-15. The F-15 would then be able to safely carry the wing to the limit of its envelope.

Such an approach presented several immediate constraints. The wing had to be designed such that it would incur flutter for a flight condition at which the F-15 could safely and easily operate. Also, the wing had to be designed such that it could easily mount to the Flight Test Fixture. Furthermore, the wing had to be designed such that its destruction from flutter would not cause any associated damage to the F-15 or Flight Test Fixture.

Several limitations in the physical realization of the wing resulted from these constraints. The main limitation was in the type of materials allowed in the construction. The wing was not allowed to have large metal components that might depart from the experiment and strike the F-15. The actual components needed to be frangible enough so that they could not damage the aircraft in the event of flutter. Also, the size of the wing was limited to a span of no more than 24 *in* because of space constraints between the Flight Test Fixture and the F-15 landing gear.

The flight conditions at which the wing would flutter were chosen to be Mach 0.80 and altitude of 10,000 *ft*. These conditions were chosen as a compromise between several issues. The speed was high enough so that many sub-critical test points could be flown but low enough so that transonic effects should not be strong. Also, the F-15 could easily and safely operate at these conditions.

Another constraint imposed on the system resulted from the objective of recording data for flutter prediction. Specifically, the wing needed to be excited by a deterministic command. Initial designs considered a control surface or torque tube but these were deemed too complicated and costly. The excitation system needed to be inexpensive but also satisfy the inherent frangibility constraint.

An additional and related constraint was placed on the modal frequencies of the system. The prediction of flutter depended on data from which the dynamics of the system could be analyzed. Thus, the modal frequencies needed to be low enough so that they could easily be excited and observed. The choice was made to limit the design of the wing such that the modal frequencies were less than 50 *Hz* and preferably less than 30 *Hz*.

4 Aerostructures Test Wing

4.1 Characteristics

The Aerostructures Test Wing was developed at NASA Dryden Flight Research Center. This system was designed explicitly for the purpose of demonstrating flutter during a flight test. Thus, the development was directed by the objectives and constraints associated with the project.

The ATW was initially conceived as a wing so the flutter mechanism would be realized as a bending-torsion instability. The design was an iterative process that considered structural characteristics and stability properties. This design determined the shape of the airfoil, the location of ribs and spars, and thickness and layout of the fiberglass skin. Additionally, a boom was included with the wing to provide mass balancing and alter mode shapes. The resulting structure, as shown in Figure 2, satisfied the constraints associated with modal frequencies, weight, load limits, and flutter speed.

The wing was formulated based on a NACA-65A004 airfoil shape with a 3.28 aspect ratio. The wing had a span of 18.0 *in* with root chord length of 13.2 *in* and tip chord length of 8.7 *in*. The total area of this wing was 197 *in*². The boom was a 1 *in* diameter hollow tube of length 21.5 *in*.

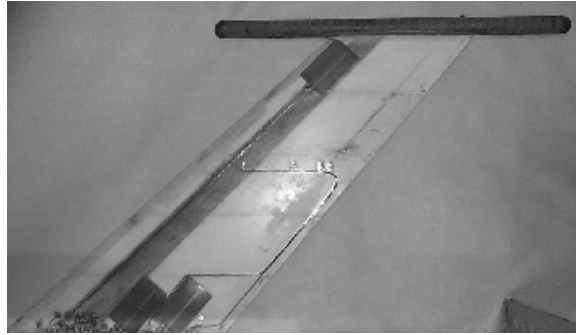


Figure 2: Aerostructures Test Wing

The ATW was meant to be a realistic testbed that represents complexity of an aircraft component; however, the construction of the testbed was limited by safety concerns. These potentially conflicting issues were addressed by designing the ATW with a rib and spar construction that used lightweight materials with no metal. Specifically, the skin and spar were constructed from fiberglass cloth, the boom was constructed from carbon fiber composite, the wing core was constructed from rigid foam, and components were attached by epoxy.

The wing has an internal spar at the 30% chord line that is constructed of carbon plies with thickness of 0.005 *in*. This spar is composed of 10 plies of carbon at the root but decreases to only 1 ply at the tip. Thus, the thickness of the spar changes from 0.05 *in* at the root to 0.005 *in* at the tip.

The total weight of the ATW was 2.66 *lb*. This weight includes the basic structural elements of both the wing and the boom. Also, this weight includes powdered tungsten that was included in the endcaps of the boom for mass balancing.

The wing was constructed with 3° of wash-in twist at the tip of the wing. The original design called for 3° of wash-out twist; however, construction errors resulted in erroneous angle of twist. This error caused some concern regarding aerodynamic and divergence issues. The concerns were alleviated by mounting the wing at a negative angle of incidence to minimize the steady-state loads for bending and torsion measured at the root and spar centerline.

4.2 Excitation and Sensing

A measurement and excitation system was incorporated into the wing¹³. This system provided data used to predict flutter and so was obviously critical to the success of the project. The design of this system was subject to the basic constraints associated with the ATW so large metal components were not acceptable. Additionally, the measurement and excitation system were required to interact with the modes of the ATW.

The measurement system was designed to provide data both for flutter prediction and loads monitoring. The ATW was constructed with 3 accelerometers placed at fore, aft and mid locations in the boom. These sensors were oriented to measure vertical responses that were perpendicular to the surface of the wing. Also, 18 strain gages were placed throughout the airfoil structure.

The excitation system was 6 patches of piezoelectric material. The wing was constructed with 3 patches on the upper surface and 3 patches on the lower surface. The same signal was commanded to these patches; however, the signal was out of phase between the upper and lower patches. In this way, the patches acted as a single

distributed actuator.

The patches were constructed as a piezoceramic encapsulated using a polymer film. Each patch had dimensions of 3 in by 1.75 in by 0.008 in. This device underwent a dimensional change when an electric voltage was applied. The patch was bonded such that this dimensional change applied a strain to the wing surface.

The orientation of the measurement and excitation system can be seen in Figure 2. The patches on this upper surface of the wing are clearly seen to be distributed with one patch near the tip and two patches near the root. The orientation of the patches and strain gages near the root are more clearly seen in Figure 3.

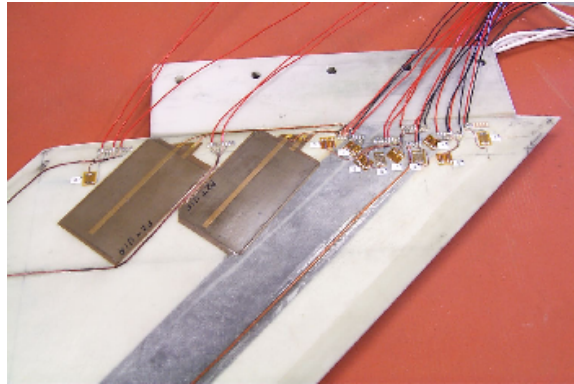


Figure 3: Instrumentation

The measurement and excitation elements were positioned to maximize their effect with respect to the bending and torsion modes. The distributed locations of the patches was such that they could act as a single actuator but still excite both bending and torsion. This ability can be seen in Figure 2 by noting the patches were aligned along the sweep angle of the wing to excite bending but they were placed at different chord-wise positions to excite torsion. The accelerometers were simply positioned along the boom to maximize response levels from both bending and torsion based on experimental testing.

4.3 Electronics

Several electronic components needed to be built to run the measurement and excitation on the ATW. These components were responsible for providing a stable power source for the different patches and sensors. Also, these components were responsible for providing an interface between the pilots and the ATW that determined the operation of the system. The components were an amplifier box, a control computer, and an interface panel shown in Fig. 4.

The control computer is shown on the left of Figure 4. This box was developed to provide an excitation signal to the piezoelectric patches on the wing. The small computer had the capability to output an analog signal with magnitudes between $+/- 10V$. The computer dimensions were 5.5 in by 5.5 in by 6.0 in.

The amplifier is shown in the middle of Figure 4. This box was a switching amplifier that could switch power supply into load at high rate and could recover the reflective energy from the capacitive loads. It had a single channel with a gain of 20 V/V for inputs up to $+/- 10 V$. The maximum output voltage was $+/- 200 V$. The maximum capacitive load capability was 100 Hz at 15 μF and 20 kHz at 1 μF . The amplifier was 8 in by 10.75 in by 3.75 in and weighed about 4 lbs.



Figure 4: Electronics

The interface panel is shown on the right of Figure 4. This small panel had 5 toggle switches that activated sweeps to the piezoelectric patches. Each switch corresponded to a sweep of different magnitude. Also, a main power switch was included that enabled a sweep to be instantly stopped so no excitation was commanded to the patches.

These components were mounted at various locations to meet space constraints. The interface box obviously had to be mounted in the cockpit. Specifically, this box was installed in the rear portion of the cockpit to allow the backseat pilot to control the operation of the ATW. The amplifier and control computer were mounted inside the Flight Test Fixture.

4.4 Mounting

The ATW mounted horizontally on the Flight Test Fixture as shown in Fig. 5. Specifically, the wing was mounted near the bottom and the nose section of the Flight Test Fixture. The system attached to the F-15 such that the ATW lay on the port side of the aircraft.



Figure 5: Aerostructures Test Wing mounted to Flight Test Fixture

The location of the wing on the Flight Test Fixture was chosen for several reasons. Mounting the wing near

the nose attempted to use the smoothest part of the airflow as indicated by previous flow visualization studies. Mounting the system near the bottom increased the distance between the wing and the fuselage which was important to minimize any interference effects from the fuselage on the ATW.

Safety was an additional concern with respect to the mounting of the ATW. Maximizing the distance between the wing and the fuselage attempted to minimize the possibility that portions of the ATW could contact the F-15 if flutter was encountered. Of course, the actual location of the Flight Test Fixture was important to this consideration. The entire system, Fixture and ATW, was mounted behind the engine inlets to minimize the possibility that destruction of the ATW could cause significant damage to the engines.

The actual connection between the ATW and the Flight Test Fixture was accomplished by constructing a new panel for the store. This panel had a slot through which a flange on the root of the ATW was inserted. Bolts fixed the flange, and consequently the ATW, to a mounting bracket on the back of the panel. This connection was quite strong so that ground testing indicated no appreciable freeplay of the ATW at the root. The connection was also shown to be quite rigid so the root of the ATW could be assumed to be fixed.

An additional feature of the panel was an ability to rotate the mounting bracket before flight. This rotation allowed the angle of incidence of the ATW to be altered. In effect, the angle of attack associated with the ATW would be changed by rotating the angle of incidence. Such rotation was used to ensure the ATW experienced small angles of attack during testing to minimize loads. The actual rotation angle was altered between flights during the testing to reflect the changes in trim angle of attack as a function of dynamic pressure.

5 Ground Vibration Test

Ground vibration tests were conducted to determine the structural dynamics of the wing. These tests were performed on the ATW mounted to a rigid stand and mounted to the Flight Test Fixture on the F-15. The difference in results was negligible so the structural properties of the ATW were assumed to be similar on the ground and in flight.

A ground vibration test was performed using a calibrated impact hammer for excitation¹⁴. This hammer used a metal tip with an added 0.0065 *lb* mass. The procedure was to impact the wing at 35 points at the leading and trailing edges, forward and aft of the spar, the wing root, the wing to boom connection, and the along the boom. The responses from these impacts were recorded by the accelerometers in the boom.

A ground vibration test was also performed using the piezoelectric excitation system¹³. This test commanded chirp signals from 5 to 35 *Hz* to generate a broad spectrum of energy. The magnitude of the chirps were varied to identify nonlinearities; however, the system appeared to be fairly linear.

The main modes of the system and their natural frequencies are presented in Table 1. These modal properties correspond to data from both the impact testing and patch testing.

Mode	Frequency (<i>Hz</i>)
1 st Bending	14.05
1 st Torsion	22.38
2 nd Bending	78.54

Table 1: Measured structural modes of the ATW

6 Modeling

The flutterometer is a state-space model-based analysis tool and, consequently, the formulation of a model was of paramount importance. A standard method is to first generate a finite element model that represents the structure, compute unsteady aerodynamics using approaches such as doublet lattice theory, and then formulate a state-space model using rational functional approximations. This standard method was initially adopted for the ATW; however, there were several unexplained sensitivity and conditioning issues. For instance, minor alterations in mass of the structure resulted in extremely large variations in predicted flutter speed. Also, the model was unable to simultaneously match both the natural frequencies and mode shapes as measured by the ground vibration test. Consequently, the finite element model was not used for flutterometer development.

An approach was used to generate a model of the ATW that combined elements from a finite element model with data from the ground vibration testing. A finite element model was initially used to generate a set of mass values at locations throughout the structure. Correspondingly, the test data indicated the frequencies and responses at these locations for modes of the structure. An equivalent model was then formulated with natural frequencies and modes shapes that were determined by the data, mass values that were purely analytical, and stiffness values that resulted from relating the analytical mass and experimental natural frequencies. This equivalent model was thus representative of both analytical and experimental results. This model was formulated using the ZAERO package¹⁵.

The first use of the equivalent model was to generate a state-space representation of the structural dynamics of the ATW. This representation resulted from generating a reduced-order model of mass and stiffness values that were associated with the modes of Table 1. The equivalent model did not use any structural damping so a modal damping matrix was determined directly by the test data. This determination was a straightforward procedure based on system identification results.

Also, the structural model was augmented to include the excitation and sensing elements. An input matrix was generated that noted the effects of the excitation system on the structural dynamics. Similarly, an output matrix was generated that noted the responses of the accelerometers throughout the structure. Each of these matrices was identified directly from the data of the ground vibration test. These matrices were generated with a relatively high amount of confidence because the excitation system is actually a structural excitation system that affects strains and stresses rather than an aerodynamic excitation system such as control surfaces. Thus, the input and output matrices could be completely determined entirely from ground vibration testing.

The quality of the structural model was evidenced by comparing transfer functions from the model and the test data. These transfer functions related the input command to the excitation system and the output responses from the accelerometers in the boom. Figure 6 compares transfer functions from model and data for the accelerometer at the trailing-edge of the boom. This comparison demonstrated that the structural model was able to accurately reproduce the dynamics as observed in the data.

The second use of the equivalent model was to generate a state-space representation of the unsteady aerodynamic forces. The equivalent model was used directly by standard computational tools to compute the aerodynamic forces and flutter speeds. These forces were computed as a set of complex matrices for a set of distinct reduced frequencies. A state-space representation of the forces was then generated by approximating the set of matrices as a rational function¹⁶.

The analysis of the equivalent model resulted in a state-space model of the structural dynamics and a state-space model of the aerodynamics. These models needed to be altered to fit into the μ -method framework and also combined to generate an aeroelastic model. This procedure was quite straightforward as documented in the literature¹⁷. The model was put into the μ -method framework by parameterizing the elements around flight

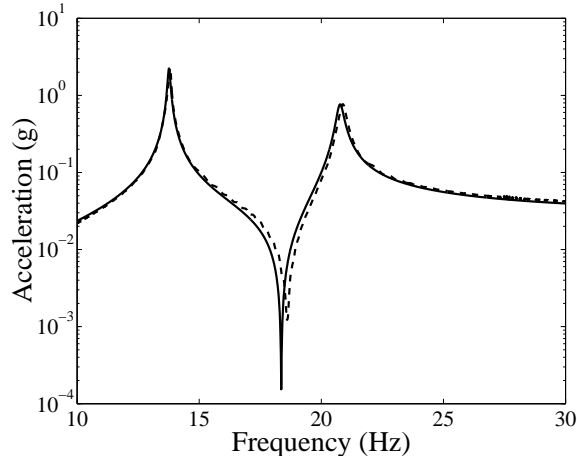


Figure 6: Transfer functions from excitation system to accelerometer at boom trailing-edge for data (---) and model (—)

condition and adding uncertainties. Then, the generation of a single aeroelastic model was accomplished by relating the structural and aerodynamic models by feedback.

The parameterization around flight condition was accomplished by noting the dependence of the aerodynamics on airspeed. The concept was to replace the airspeed parameter with a summation of a nominal airspeed and a perturbation. The explicit dependence of the dynamics on this perturbation was then replaced by an equivalent dependence through feedback for the nominal value and the perturbation.

The introduction of uncertainties actually made use of both the structural and aerodynamic representations. One type of uncertainty that was introduced was parametric uncertainty. Uncertainty operators were directly associated with the stiffness and damping matrices of the structural dynamics. Another type of uncertainty that was introduced was dynamic uncertainty. This type of uncertainty was associated with the magnitude and phase of the aerodynamic forces. Also, dynamic uncertainty was associated with the excitation and sensing signals to account for the effects of unmodeled dynamics and mode shape errors.

The aeroelastic model in the μ -method framework is shown in Figure 7. The elements of this model are easily seen. In particular, the structural dynamics are noted as S and the aerodynamics are noted as A . The perturbation to airspeed, δ_V , appears in association with the aerodynamics because that block contains all the velocity dependency. Also, the parametric and dynamic uncertainties are shown in relation to the elements with which they are associated. The elements Δ_K and Δ_C are the parametric uncertainties associated with stiffness and damping, Δ_A is the dynamic uncertainty associated with the aerodynamic forces, and Δ_i and Δ_o are the dynamic uncertainties associated with input and output signals. Note that each of these operators is weighted to reflect a desired level of uncertainty. For example, the operator Δ_K is restricted to be norm bounded by unity so the weighting W_K scales the loop and allows consideration of errors that are not of unity size. The actual values of the weightings were determined by analysis of flight data.

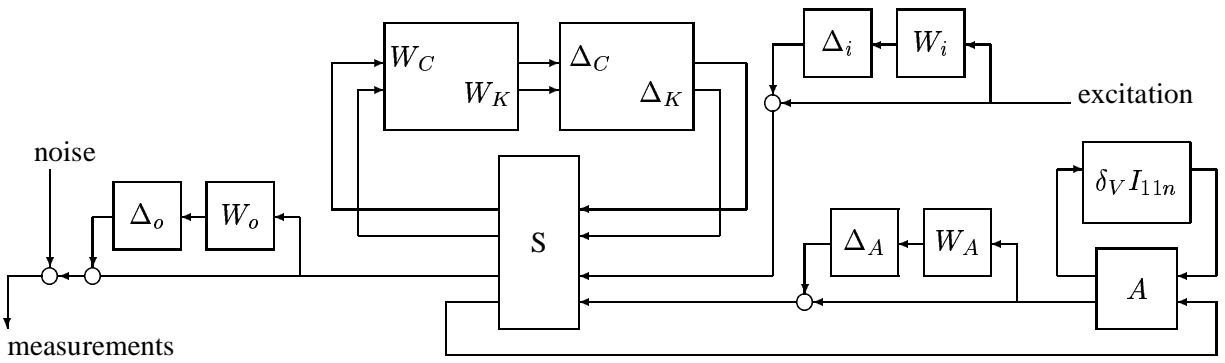


Figure 7: Uncertain model of the Aerostructures Test Wing

7 Flight Test

7.1 Envelope Expansion

The ATW was first flown during March 2001 at NASA Dryden Flight Research Center as shown in Fig. 8. The mass balancing in the boom for this flight was chosen such that the flutter speed was excessively high for the ATW. Thus, the initial flight was used to test the system and procedures with the wing in a relatively safe flight configuration. After this flight, the mass was changed so the system was anticipated to flutter near Mach 0.80 and altitude of 10,000 *ft*.



Figure 8: Flight test of the ATW

The ATW, in its final configuration, was flown on 4 flight tests during April 2001. These flights included 21 test points with Mach numbers between 0.50 to 0.83 and altitudes between 10,000 and 20,000 *ft*. The test points were chosen in an order of varying Mach and altitude such that the envelope expansion always increased dynamic pressure.

An interesting aspect of the flight test was takeoff and landing. These maneuvers are, of course, characterized by deployment of the landing gear. The flow conditions around the Flight Test Fixture, and consequently the ATW, were strongly affected by the landing gear. The ATW experienced strong buffeting during these flight conditions such that accelerometer responses reached the 25 *g* saturation limits of the telemetry recording. The pilots minimized the time spent in this dangerous buffet by retracting the landing gear immediately after takeoff

and extending the gear at the last safe moment before touching down.

The flight test for envelope expansion followed standard procedures for test point operation. Specifically, the aircraft arrived on condition and then flew straight and level for 30 seconds to gather information about turbulence levels. After the stabilized run, the excitation system on the ATW was activated and response data was measured. This response data was telemetered to the control room and analyzed by damping and flutterometer algorithms. Also, wind-up turns and push-over/pull-up maneuvers were performed to gather information about loads on the ATW.

The decision to repeat a test point was made by inspection of the flight data. Essentially, the data was analyzed both in the time domain and frequency domain to determine if sufficient information about the dynamics could be observed. The time domain check simply inspected the magnitude of the accelerometer data to ensure adequate levels of response were observed. The more methodical check was analysis of the frequency-domain transfer functions. The test point was repeated if the data showed unacceptably small responses or contained excessively high levels of noise that distorted the transfer function and resulting damping estimation.

Also, the test points at high speeds needed to be considered particularly carefully before expanding the envelope. The flight corridor within which the ATW was required to operate was not long enough to ensure a full 60 s chirp excitation could be completed at Mach 0.80. The flutter prediction really only required modal information so the test point was considered sufficient if the excitation was able to excite the bending and torsion modes. Since the torsion mode was always less than 25 Hz, the first 45 s of the chirp were sufficient to complete the test point.

The flight test proceeded as the control room decided to continue expanding the envelope between test points. This decision was predominantly based on the desire to closely approach, but hopefully not encounter, the onset of flutter. The flutterometer and damping trends were both used to predict how close the system was to instability.

The envelope expansion was actually only partially limited by the prediction of flutter onset. Traditionally, of course, the expansion would stop when the system was deemed to be near unstable flight conditions. The purpose of the flight test for the ATW was to take the system very close to flutter; therefore, the expansion continued until the flight conditions associated with flutter were confidently determined.

7.2 Flutter

The ATW experienced the onset of flutter during an envelope expansion. Specifically, the system was being accelerated after the final test point at Mach 0.825 and altitude of 10,000 ft. The pilot was doing a very slow acceleration of approximately .01 Mach per second at constant altitude. The onset of flutter occurred at approximately Mach 0.83 and altitude of 10,000 ft.

Photos were taken from the video system that showed the onset of flutter. Several photos, taken 0.033 s apart, are shown in Fig. 9. The wing underwent several violent oscillations until it broke near the tip. The boom and roughly 20% of the wing were lost.

The actual flutter mechanism is seen from the photos in Fig. 9. The unstable mode is clearly dominated by bending motion. Some torsion is evident as would be expected by the anticipated modal coupling between the modes. The actual mode shape associated with the flutter mechanism was somewhat difficult to determine because the large oscillations quickly caused damage to the system so the photographed response may not exactly correlate to the original linear structure.

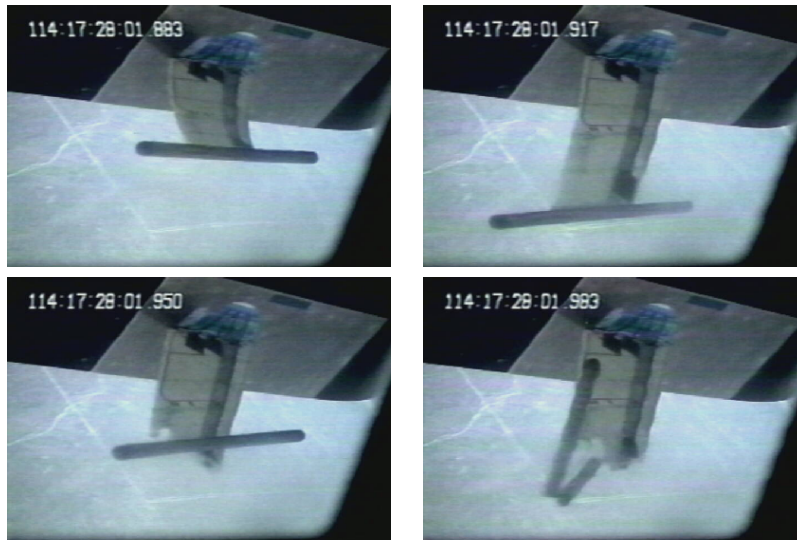


Figure 9: Onset of flutter

The rapidity at which the ATW was destroyed is particularly interesting. Essentially, the wing was destroyed about 2 s after the onset of flutter was observed. The project had hoped to save the wing after the flight conditions associated with flutter were confidently determined; however, the destruction occurred so fast that the wing could not be saved. The control room quickly made the abort call to the pilot when flutter was observed but simply saying the words took roughly the same amount of time as the destruction.

Even more disturbing, the control room was clearly aware that flutter was imminent but was still unable to stop the destruction. The data analysis showed levels of modal damping for the bending mode were changing to indicate flutter was probable near this flight condition. The exact condition was difficult to confidently determine so the envelope was being expanded very slowly. The flutter experienced by the ATW was so severe that even alert and forewarned monitoring was unable to prevent loss of the system.

The status of the host F-15 aircraft was of obvious concern after the ATW experienced flutter. The pilot reported no adverse effects were observed. The chase pilot flew around the F-15 for visual inspection and also reported no adverse effects could be observed. The video shows the destroyed parts of the ATW fell away harmlessly without contacting the F-15 after flutter. Thus, the system behaved as predicted by the methodical and extensive analysis performed by the design team and flight engineers associated with the ATW.

8 Predictions of Flutter Speed

8.1 Implementation

The flutterometer was implemented for ATW testing as a MATLAB process. In actuality, there were several processes that operated in conjunction. The flutterometer, as referred to in this paper, implies the process that computed on-line robust flutter margins. The other processes dealt with data transfer. Essentially, the processes operated independently; however, the proper operation of the flutterometer depended on an implementation that allowed these processes to communicate efficiently.

The overall flowchart for the flutterometer implementation traces the data from aircraft telemetry to the generation of a robust flutter margin. This flowchart has many steps; however, the implementation can effectively be viewed as 3 steps.

The first step in the flutterometer implementation was to gather data from the aircraft telemetry stream. This step was done using a framework for data networking called the ring buffered network bus (RBNB)¹⁸. The concept used for ATW testing had an RBNB process transferring data from the telemetry stream to a memory cache. The data in the cache was converted from generic telemetry units, such as counts, into engineering units, such as acceleration in g , for use with analysis processes. Also, the cache contained all signals from the entire flight. In this way, the cache acted like an on-line data server from which any data that was gathered during the flight could be immediately accessed.

The second step in the implementation was to provide an interface that linked the data server with MATLAB. This software was written as a MATLAB process that ran continuously and monitored the data cache. The concept behind this process was to poll the data until a condition was satisfied that indicated data should be transferred. This trigger condition for the ATW testing was a signal that was nonzero only while the excitation system was active. The interface process transferred a block of data, corresponding to a continuous stream of data with a nonzero excitation signal, between the data cache and the local analysis computer. Also, the interface system converted the data from an RBNB format into a MATLAB structure. The data was then saved as a file with a unique identifier that corresponded to the time at which the data was generated.

The third step was to analyze the data and compute a robust flutter margin. This step was the flutterometer process and was entirely a MATLAB function. The process began by loading a user-specified data file. The flight conditions associated with the data file were noted and a corresponding model was loaded. The process then continued by generating uncertainty levels and performing a μ analysis to compute an on-line flutter margin.

The interaction between the user and the implementation was only in the third step. The first and second steps were initialized with information about the telemetry stream and the trigger condition and then run autonomously. The third step was not as deterministic and thus was required to be monitored. Some of the parameters that were allowed to be changed during a flight were the frequencies for model validation and μ analysis, the updating scheme for the uncertainty levels, the flight condition units of the flutter margin, the sensors to be considered for analysis, and various display options. The flutterometer employed an interface that allowed these options to be changed by simple graphical entries.

8.2 Flight Data

The responses from the accelerometers were used to predict the onset of flutter. The time-domain responses were used for evaluation of the aeroelastic dynamics; however, these responses were further processed. In particular, the data was represented as frequency-domain responses for several types of analysis.

The basic frequency-domain representation of the data was transfer functions. These transfer functions were computed between the commanded excitation and the accelerometer responses. Obviously transfer functions could not be computed for the responses to turbulence excitation so frequency-domain representations of these responses were computed as power spectra.

Estimates of modal parameters were computed from the transfer functions. At each test point, a polynomial-basis curve-fit method of system identification was used to formulate a model whose magnitude and phase characteristics were similar to the transfer function. The modal parameters of that model were then extracted

and used as representative of the ATW parameters.

The modal dampings that were extracted at each test point are given in Fig. 10. The flutter instability affecting the bending mode is clearly evident in the data trends. Furthermore, the damping data indicates that the ATW experiences a classical type of flutter such that one mode is becoming less stable while the other mode is becoming more stable¹⁹.

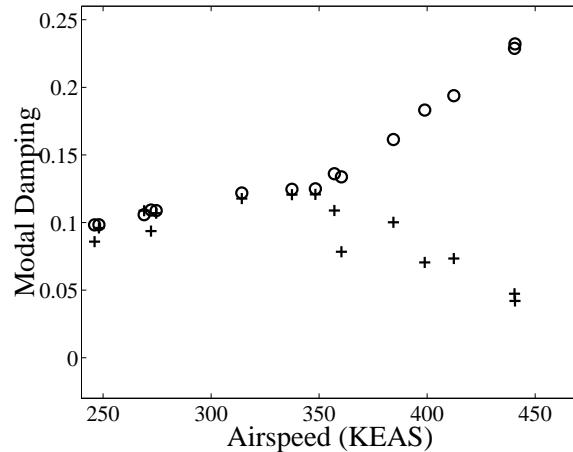


Figure 10: Measured modal dampings for bending mode (+) and torsion mode (o)

The modal frequencies for the ATW are given in Fig. 11. This data seems to contradict the notion that the ATW is experiencing a classical bending-torsion flutter. Notably, the natural frequencies do not appear to be coalescing, as is sometimes expected for classical flutter, until a possible coalescence at the airspeed very close to the onset of flutter. Instead, the flutter mechanism for the ATW is a binary flutter with limited frequency coalescence.

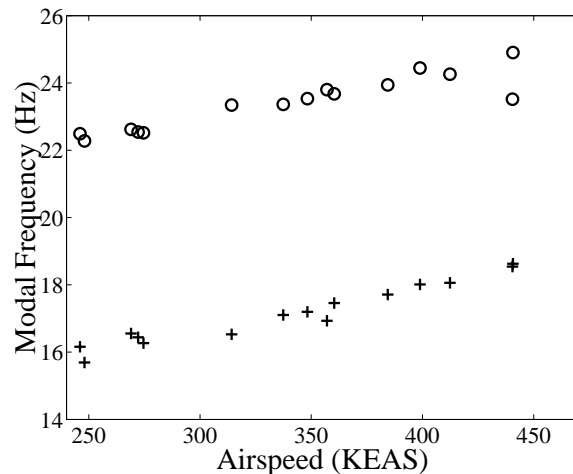


Figure 11: Measured modal frequencies for bending mode (+) and torsion mode (o)

An issue to note in Fig. 10 and Fig. 11 is that only 15 estimates are shown even though the flights operated at 21 test points. Some estimates are missing because the responses from several of the test points were unable to present sufficient information about the bending mode. The response levels were quite low at these test points

so accurate modal estimates could not be obtained. The reason for the poor data quality at some points was unclear but possibilities included high levels of turbulence and noise or unexplained high damping.

Finally, several types of data were available for analysis to predict the onset of flutter. This first type of data was simply the time-domain responses of the accelerometers. Another type of data was the corresponding frequency-domain responses computed by standard Fourier techniques. Additionally, a 4-state model was available from system identification techniques applied to the frequency-domain data between 12 Hz and 30 Hz .

8.3 Model Updating

The analytical model, which includes the theoretical dynamics and associated uncertainty description, needed to be updated at each test point. This updating actually altered different parts of the model. The initial change to the model involved altering coefficients in the equations of motion for the theoretical dynamics. The other change was to alter the uncertainty associated with those dynamics.

The change to the theoretical dynamics was accomplished using a modal approach. Essentially, the dynamics associated with each aeroelastic mode were separated and independently updated. These updates changed the damping and natural frequency of the mode along with the observability of the states.

The largest update to the model was alterations to the modal observability. The magnitude and phase of response from each mode was considerably different between the model and the data. There were also updates to the damping and natural frequency but the observability was clearly the dominant error. The transfer functions of the flight data, the original model, and the updated model are shown in Fig. 12 for the flight condition of Mach 0.60 and 20,000 ft .

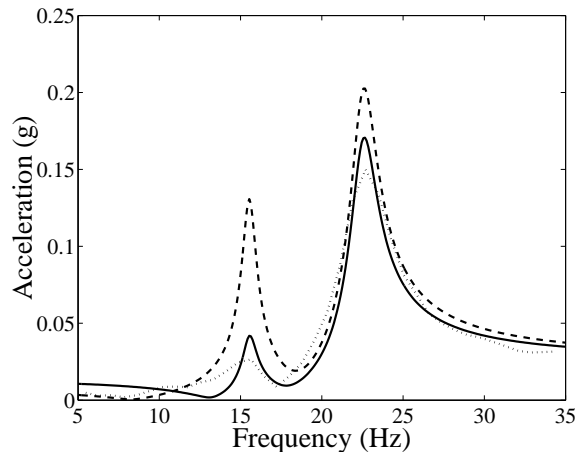


Figure 12: Transfer functions from excitation to accelerometer for data (...), model with original observability (- - -), and model with updated observability (—)

This update to the observability was made uniformly to the theoretical models at every test point. This type of update is not the optimal way to develop models but it was a straightforward method to formulate reasonable models. The underlying cause of the error in the theoretical models was never determined but was assumed to be an incorrect mode shape resulting from inaccuracies in computational calculations of the aerodynamic forces.

The uncertainty description was also updated at each test point. This description accounts for differences

between the theoretical and measured transfer functions. The initial updates to the modal dynamics clearly reduced these differences as shown in Fig. 12. Thus, the uncertainty associated with the updated model was considerably less than the uncertainty associated with the original model. The actual magnitudes of the uncertainty were computed automatically using the process of model validation for uncertain systems.

8.4 Flutter Speeds

Flutter speeds were predicted at each test point during the envelope expansion. The basic concept was to make use of flight data available from any of the previous test points to make these predictions. The approaches used during the flight tests were extrapolating damping trends and the flutterometer. These predictions were only computed during the 4 flights of the ATW in its final configuration because, as stated earlier, the initial flight was mostly for system validation rather than data generation and flutter prediction.

The approach to predict the onset of flutter by extrapolating damping trends was a traditional method commonly used for envelope expansion ¹. In this case, the trends corresponded to damping values obtained from the analysis of the frequency-domain data as shown in Fig. 10. The damping trends were analyzed by visual inspection and curve fitting to determine the speed at which damping indicated instability.

The other approach to predict the onset of flutter was the flutterometer. This tool also utilized the frequency-domain data; however, the modal dampings and frequencies were not of direct interest. The flutterometer compared the transfer functions between the theoretical model and the flight data to determine errors in that model. The resulting uncertain model was evaluated using μ -method analysis to compute a robust flutter speed.

The predictions of flutter speed were computed as knots of equivalent airspeed (*KEAS*). The use of these units allowed the prediction to avoid issues of Mach and altitude dependence. The ATW was assumed to flutter near Mach 0.80 and altitude of 10,000 *ft* so the flutter speed reflected variations around that condition.

The first flight of the ATW for envelope expansion only operated at 5 test points with speeds up to 274 *KEAS*. The initial predictions of flutter speeds during this flight were quite different based on damping trends and flutterometer. Specifically, the damping trends were unable to predict a reasonable value of flutter speed whereas the flutterometer immediately predicted a speed of 405 *KEAS*.

The reason for the difference in predicted speeds was quite easy to determine. The damping trend was based on the values shown in Fig. 10 for low-speed test points. Obviously the damping values showed little variation across these points so a trend could not be observed that indicated flutter. Conversely, the flutterometer had an inherent prediction of flutter speed from the theoretical model so the flight data was used to update that prediction. The result of this prediction from a combination of model and data was a speed that was conservative but still reasonably close to the anticipated value.

The second flight for envelope expansion began by covering test points with speeds around 300 *KEAS*. Initially, the flutter speeds predicted during this flight were similar in nature to the predictions from the first flight. The extrapolation of damping trends generated widely scattered predictions for these points much like those generated during the first flight. Also, the flutterometer predicted the same speed of 405 *KEAS* during this flight to match its predictions during the first flight.

The second flight concluded by generating data from test points with speeds up to 356 *KEAS*. The predictions from the flutterometer remained at 405 *KEAS*; however, the predictions from the damping extrapolation changed dramatically. The damping values for the bending mode were seen in Fig. 10 to noticeably change for flight conditions with airspeed greater than 350 *KEAS*. This change indicated the onset of flutter. Thus, the damping

trend could be extrapolated and a reasonable prediction of flutter speed resulted.

The third flight for envelope expansion repeated test points at 2 conditions from the previous flight and then expanded the envelope using test points at 6 new flight conditions up to 438 *KEAS*. The speeds predicted by the flutterometer remained unchanged at 405 *KEAS* whereas the speeds predicted by damping extrapolation converged to roughly 460 *KEAS*.

The final flight for envelope expansion used only 1 test point at 445 *KEAS*. The data from this test point was analyzed by the prediction algorithm. The flutterometer still predicted 405 *KEAS* and the damping extrapolation predicted 470 *KEAS*.

The actual predictions of flutter speed are shown in Fig. 13. The predictions from the damping trends are clearly shown to vary widely as the flights began but converged to the correct solution. The predictions from the flutterometer are also clearly shown to remain constant throughout the flight testing.

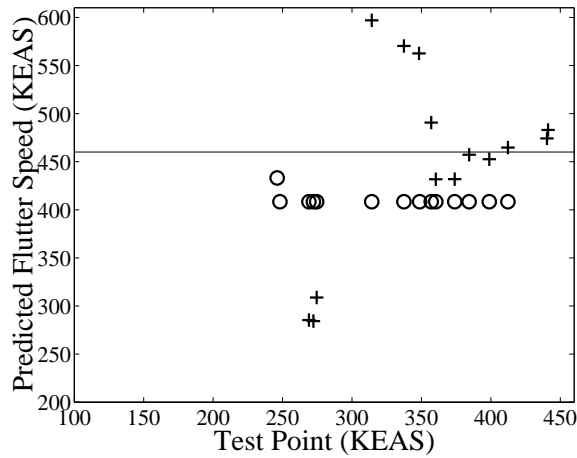


Figure 13: Predicted flutter speeds during envelope expansion from damping trends (+) and flutterometer (o)

The predictions shown in Fig. 13 should be noted with some consideration as to their computation. Specifically, the speeds predicted by extrapolating damping trends were actually somewhat arbitrary. Several procedures were used to extrapolate the trends and resulted in predictions that varied by up to 30 *KEAS*. Furthermore, several techniques were used to estimate damping²⁰. The predictions shown in Fig. 13 result from a standard second-order curve fit to the damping values of Fig. 10. During the flight, the envelope expansion needed to accept these predictions along with some level of variation that made a definitive prediction nearly impossible from damping trends.

9 Evaluating the Flutterometer

The ability of the flutterometer to predict the onset of flutter was demonstrated by this experiment. An evaluation of the tool could certainly be made by comparing the predicted speeds for flutter to the actual speed at which flutter occurred. This evaluation was strengthened by comparing the abilities of the flutterometer to the abilities of extrapolating damping trends.

An interesting comparison between the flutterometer and damping trends was seen in Fig. 13. The predictions from damping extrapolation were initially quite poor but eventually converged to the correct speed. The pre-

dictions from the flutterometer were initially conservative but did not converge to the correct speed despite the additional data provided as the envelope was expanded. The high variation in the predictions from extrapolating damping trends was easily explained by considering the damping values in Fig. 10 but the low variation in the predictions from the flutterometer resulted from other causes ²¹.

The prediction of flutter based on the flutterometer was dependent on uncertainties in the model. The data from the initial test point was actually sufficient to indicate these errors. The data from additional test points did not indicate any further errors. Thus, the amount of modeling error did not change as the envelope was expanded. Correspondingly, the predicted flutter speed did not change because nothing about the uncertain model was changing. This behavior was shown by the speed predicted by the flutterometer in Fig. 13 remaining unchanged as the envelope was expanded.

The values of the predictions were especially interesting when viewed in the context of the flight tests. The damping extrapolation provided no useful information for the entire first flight and most of the second flight. In fact, this method was really only useful during the third and fourth flights. The flutterometer, conversely, was quite informative immediately during the first flight but was actually of decreasing value as the envelope expanded. In fact, the third and fourth flights expanded the envelope beyond the flutter speed predicted by the flutterometer.

The inability of the flutterometer to converge to the correct solution was actually a result of model updating. The flutterometer was programmed to only update the uncertainty description such that the theoretical dynamics were never changed. The basic change of updating the observability was straightforward but any further updating of the theoretical model was difficult and unreliable because of inconsistent observability in the data.

Furthermore, the uncertainty levels were never allowed to decrease. This approach was also related to the inconsistent observability in the data. The basic premise was that an error might have been present in the model but only certain test points were able to observe that error. This approach was meant to maximize safety and conservatism by ensuring an error, once observed, would always be associated with the model.

Also, the flutter predictions approaches are actually formulated to be theoretically valid for envelope expansion at constant Mach but increasing airspeed. The actual flight test had to consider expansion using test points with varying Mach. This type of expansion caused some concern with respect to relying on the flutter predictions but it was necessitated by practical constraints. As the data shows, the effect of varying Mach was not dramatic and the flutter predictions were indeed reasonable.

10 Post-Flight Analysis

The flutterometer was demonstrated to be conservative; however, that conservatism could be considered excessive for some applications. The data from the ATW was used to continue research into the prediction of flutter. In particular, the data was used to formulate an augmented flutterometer that predicted the flutter speeds with less conservatism than the original implementation.

The flutterometer was augmented by including processes for signal processing and parameter estimation. The signal processing involved eliminating high-order components of the data. This processing was essentially an optimal filter that resulted by extracting the linear components of the data via a Volterra kernel ²². The parameter estimation involved computing optimal updates to the modal dynamics. The actual implementation used a running average of the updates at all flight conditions to ensure only consistent errors were eliminated.

The flutterometer predictions resulting from the augmented implementation are shown in Fig. 14. The new

implementation predicts flutter speeds that are very close to the true speed. In fact, the flutterometer is able to predict the onset of flutter to within 10 *KEAS* using data from any point in the flight test.

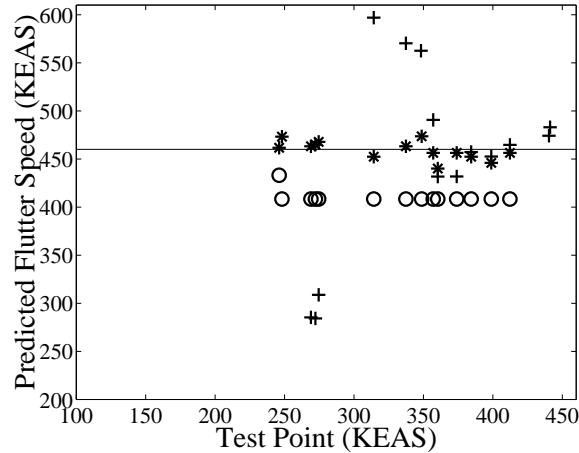


Figure 14: Predicted flutter speeds during envelope expansion from damping trends (+) and original flutterometer (o) and augmented flutterometer (*)

The flutterometer has clearly been demonstrated to be a valuable tool for flight testing. The original implementation used a worst-case approach that maximized safety but also maximized conservatism. The new implementation relies more heavily on measured data properties so it slightly reduces the safety factor but correspondingly reduces the conservatism.

The data from the ATW is being used to incorporate several methods of model updating for the flutterometer. One such approach that is being adopted is a formal routine for system identification that simultaneously computes observability parameters and their uncertainties²³. Also, the investigation into nonlinear dynamics is being pursued by analyzing the second-order Volterra kernel extracted from the flight data.

11 Conclusions

The Aerostructures Test Wing was a successful experiment. Flight tests of the ATW were indeed able to demonstrate flutter. The system was designed such that the onset of flutter caused destruction of the experiment but caused no damage to the host aircraft. This experiment has shown that such tests can be safely performed by carefully designing a system and flight program that accounts for the potential hazards that may be encountered.

Data recorded during these flights have been used to predict the onset of flutter and demonstrate strengths and weaknesses of the corresponding prediction methods. In particular, the methods of extrapolating damping trends and flutterometer were investigated. The predictions from the damping method were initially poor but improved dramatically as the envelope was expanded. Conversely, the predictions from the flutterometer were initially slightly conservative but remained so throughout the flight testing even though more data was gathered.

These results indicate a method to perform envelope expansion. The flight test should be initiated using the flutterometer at the low-speed test points to get an initial conservative estimate of the flutter speed. The test would proceed using the flutterometer estimates until the test points approach the predicted speed. The envelope expansion at high-speed conditions should rely more heavily on the data-driven methods to finalize an accurate prediction of the exact speed at which flutter will be encountered. Of course, the envelope expansion must still

proceed with extreme caution but possibly the combination of these approaches will allow for a more efficient flight test program.

References

- [1] Kehoe, M.W., *A Historical Overview of Flight Flutter Testing*, NASA-TM-4720, October 1995.
- [2] Livne, E., "Integrated Aeroservoelastic Optimization: Status and Direction," *Journal of Aircraft*, Vol. 36, No. 1, January-February 1999, pp. 122-145.
- [3] Battoo, R.S., "An introductory guide to literature in aeroelasticity," *The Aeronautical Journal*, November 1999, pp. 511-518.
- [4] Cooper, J.E., Emmett, P.R., Wright, J.R. and Schofield, M.J., "Envelope Function - A Tool for Analyzing Flutter Data," *Journal of Aircraft*, Vol. 30, No. 5, September-October 1993, pp. 785-790.
- [5] Zimmerman, N.H. and Weissenburger, J.T., "Prediction of Flutter Onset Speed Based on Flight Testing at Subcritical Speeds," *Journal of Aircraft*, Vol. 1, No. 4, July-August 1964, pp. 190-202.
- [6] Nissim, E. and Gilyard, G.B., *Method for Experimental Determination of Flutter Speed by Parameter Identification*, NASA-TP-2923, June 1989.
- [7] Girard, M. and McIntosh, S., "Flutter Testing in the 90's (The GBU-24 Saga)," *Proceedings of the IEEE Aerospace Conference*, Institute of Electrical and Electronics Engineers, Piscataway, NJ, 1998, Vol. 3, pp. 39-50.
- [8] Dunn, S.A., Farrell, P.A., Arms, P.B., Hardie, C.A., and Rendo, C.J., "F/A-18A Flight Flutter Testing - Limit Cycle Oscillation or Flutter," *Proceedings of the International Forum on Aeroelasticity and Structural Dynamics*, Asociacion de Ingenieros Aeronauticos de Espana, Madrid Spain, 2001, Vol. 3, pp. 299-310.
- [9] Lind, R. and Brenner, M., "The Flutterometer : An On-Line Tool to Predict Robust Flutter Margins," *Journal of Aircraft*, Vol. 37, No. 6, November-December 2000, pp. 1105-1112.
- [10] Lind, R. and Brenner, M., *Robust Aeroservoelastic Stability Analysis*, Springer-Verlag, London, April 1999.
- [11] Packard, A. and Doyle, J., "The Complex Structured Singular Value," *Automatica*, Vol. 29, No. 1, January 1993, pp. 71-109.
- [12] Richwine, D.M., *F-15B/Flight Test Fixture II: A Test Bed for Flight Research*, NASA-TM-4782, December 1996.
- [13] Voracek, D., Reaves, M., Horta, L. and Potter, S., "Piezoelectric Actuators for Ground and Flight Test Structural Excitation," *Proceedings of the AIAA Structures, Structural Dynamics, and Materials Conference*, American Institute of Aeronautics and Astronautics, Reston, VA, AIAA-2002-1349, April 2002.
- [14] Potter, S. and Lind, R., "Developing Uncertainty Models for Robust Flutter Analysis using Ground Vibration Test Data," *Proceedings of the AIAA Structures, Structural Dynamics, and Materials Conference*, American Institute of Aeronautics and Astronautics, Reston, VA, AIAA-2001-1585, April 2001.
- [15] Zona Technology, *ZAERO Users Guide*, Scottsdale AZ, 2000.

- [16] Karpel, M., "Design for Active Flutter Suppression and Gust Load Alleviation using State-Space Aeroelastic Modeling," *Journal of Aircraft*, Vol. 19, No. 3, March 1982, pp. 221-227.
- [17] Lind, R., "Match-Point Solutions for Robust Flutter Analysis," *Journal of Aircraft*, January-February 2002, Vol. 39, No. 1, pp. 91-99.
- [18] Freudinger, L.C., Miller, M.J., and Kiefer, K., "A distributed computing environment for signal processing and systems health monitoring," *Proceedings of the AIAA/IEEE/SAE Digital Avionics Systems Conference*, American Institute of Aeronautics and Astronautics, Reston, VA, October 1998, pp. C35/1-C35/8.
- [19] Hancock, G.J., Wright, J.R., and Simpson, A., "On the Teaching of the Principles of Wing Flexure-Torsion Flutter," *The Aeronautical Journal*, Vol. 89, No. 888, October 1985, pp. 285-305.
- [20] Brenner, M.J., *Nonstationary Dynamics Data Analysis with Wavelet-SVD Filtering*, NASA-TM-2001-210391, April 2001.
- [21] Lind, R. and Brenner, M., "Flight Test Evaluation of Flutter Prediction Methods," *Proceedings of the AIAA Structures, Structural Dynamics, and Materials Conference*, American Institute of Aeronautics and Astronautics, Reston, VA, AIAA-2002-1649, April 2002.
- [22] Prazenica, R.J., Lind, R., and Kurdila, A.J., "Uncertainty Estimation from Volterra Kernels for Robust Flutter Analysis," *Proceedings of the AIAA Structures, Structural Dynamics, and Materials Conference*, American Institute of Aeronautics and Astronautics, Reston, VA, AIAA-2002-1650, April 2002.
- [23] Brenner, M.J., "Aeroservoelastic Uncertainty Model Identification from Flight Data," *Proceedings of the International Forum on Aeroelasticity and Structural Dynamics*, Asociacion de Ingenieros Aeronauticos de Espana, Madrid Spain, 2001, Vol. 3, pp. 299-310.